

Observable imprints of primordial gravitational waves on the temperature anisotropies of the Cosmic Microwave Background

Miguel-Angel Sanchis-Lozano and Veronica Sanz*

Departamento de Física Teórica and Instituto de Física Corpuscular, CSIC-University of Valencia

We examine the contribution of tensor modes, in addition to the dominant scalar ones, on the temperature anisotropies of the cosmic microwave background (CMB). To this end, we analyze in detail the temperature two-point angular correlation function $C(\theta)$ from the *Planck* 2018 dataset, focusing on large angles ($\theta \gtrsim 120^\circ$) corresponding to small ℓ multipoles. A hierarchical set of infrared cutoffs are naturally introduced to the scalar and tensor power spectra of the CMB by invoking an extra Kaluza-Klein dimension compactifying at about the GUT scale between the Planck epoch and the start of inflation. We associate this set of lower scalar and tensor cutoffs with the parity of the multipole expansion of the $C(\theta)$ function. By fitting the *Planck* 2018 data we compute the multipole coefficients thereby reproducing the well-known odd-parity preference in angular correlations seen by all three satellite missions COBE, WMAP and *Planck*. Our fits improve significantly once tensor modes are included in the analysis, hence providing a hint of the imprints of primordial gravitational waves on the temperature correlations observed in the CMB today. To conclude we suggest a relationship between, on the one hand, the lack of (positive) large-angle correlations and the odd-parity dominance in the CMB and, on the other hand, the effect of primordial gravitational waves on the CMB temperature anisotropies.

Keywords: Primordial gravitational waves, Cosmic Microwave Background, Temperature angular correlations, Extra dimensions

I. INTRODUCTION

In an inflationary scenario, primordial energy density inhomogeneities, due to the unavoidable quantum fluctuations of the primordial field, are the seed of the primary temperature CMB anisotropies, as well as the large scale structure of our observable universe today. Usually, temperature anisotropies are mainly attributed to the scalar modes of the inflaton field, while tensor modes are expected to be subdominant, therefore hardly distinguishable from the former. On the other hand, common wisdom usually states that polarization of the CMB remains as the main hope to detect primordial gravitational waves (PGW) produced in the very early universe [1] as only tensor -and not scalar - modes can produce B-modes of polarization [2]. Note however that disentangling B-modes of PGW from other non-cosmological sources (e.g. gravitational lensing) renders this method rather cumbersome so far. Nevertheless, future very-high precision measurements of the CMB polarization [3–5] could uncover a PGW background in this way.

In this work, we include the expected small but maybe still observable effect of the tensor modes on the CMB temperature correlations especially at large angles (low multipoles), in spite of the big uncertainties including the cosmic variance [6]. Use will be made of a parity statistic [7, 8] to highlight the long-standing apparent odd-parity preference shown by data of all three satellite missions COBE [9], WMAP [10] and *Planck* [11, 12] in the multipole analysis of the two-point correlation function. Notice that such a parity imbalance, even to a small degree, questions the large-scale isotropy of the observable universe stemming from the cosmological principle.

In fact, the standard cosmological model can be viewed as a phenomenological effective theory of an unknown underlying more general theory yet to be discovered. Discrepancies, anomalies or puzzles, which are emerging from observations with respect to a standard cosmology scenario [13–17] may have a systematic origin, or can be due to statistical fluctuations. Their persistence, however, along different probes implying uncorrelated errors, strongly suggest the need for new physics beyond the minimal standard model in cosmology and elementary particle physics.

A. Angular correlations of the CMB and the Sachs-Wolfe effect

Two categories of temperature fluctuations observed in the CMB can be distinguished according to the cosmic time evolution: (a) primary anisotropies, prior to decoupling, and (b) secondary anisotropies, developing as photons propagate from the surface of the last scattering to the observer (us). The former include temperature fluctuations

* miguel.angel.sanchis@ific.uv.es, veronica.sanz@uv.es

due to photon propagation under metric perturbations originated by inhomogeneities of the matter field at the time of recombination, the so-called Sachs-Wolfe (SW) effect. This effect shows up at rather large angles from directions in the celestial sphere, while secondary anisotropies (as well as Baryonic Acoustic Oscillations) rather affect quite small angles and have been successfully accounted for by standard cosmology.

The SW effect will play an important role in our study to account for the temperature angular distribution, showing a lack of (positive) correlations at large angle (i.e. $\theta \gtrsim 60^\circ$) together with an apparent parity imbalance. Usually, under some simplifying assumptions, a plateau is expected from this effect in the angular power spectrum at low ℓ ($\lesssim 30$), while a sawtooth shape favoring odd- ℓ peaks is actually observed, later interpreted in this paper.

B. Parity imbalance seen in the CMB

As is well known, Nature is parity violating, e.g. in the electroweak sector of the Standard Model where only left-handed fermions are active [18]. In this context, it is natural to ask whether Nature would again violate parity through some gravitational processes, and if this feature could shed light on the very early universe itself. In fact, a variety of sources of gravitational parity violation have been considered in the literature, see e.g. [19, 20]. Any of these could have left an imprint on the net helicity of the gravity wave background, namely the preferred excitation of one circular polarization over another.

In the present study we have followed a different path, started in a previous paper (see Ref. [21]) where a certain degree of parity breaking showing up in correlations at large angle of the CMB radiation was envisaged. To this end, fundamental fermionic fields (making up a composite scalar inflaton) were introduced satisfying periodic and antiperiodic conditions on a Hubble radius in real space. In this way, two distinct infrared cutoffs, associated with integer and half-integer Fourier modes of the fluctuating field, emerged as a source of parity breaking in angular correlations. In particular, a preference for odd multipoles at large angle comes out naturally in angular two-point correlations (see appendix).

In this paper we will not resort to the existence of fermionic fields as fundamental components of a composite scalar inflaton to provide the required periodic and antiperiodic conditions, as done in Ref. [21]. Rather, we shall assume that in the very early universe a pre-inflationary scalar field satisfies certain boundary conditions on an extra spatial dimension *à la Kaluza-Klein* (just one for simplicity), to be addressed in more detail in section IV. Thereby, distinct comoving scales for infrared cutoffs (commonly related to the inverse radius of an extra dimension compactified as a circle) come into play in temperature angular correlations for both scalar and tensor modes.

In this regard, the power spectrum itself, defined by the Fourier transform of the primordial fluctuation spectrum, is often parameterized as

$$P^S(k) = A^S \left[\frac{k}{k_*} \right]^{n_s-1} \quad (1)$$

where n_s is the scalar spectral index and k_* the pivot scale. The above spectrum, referred exclusively to scalar modes, would be perfectly scale free (i.e. $n_s = 1$) if the Hubble parameter H_{inf} were strictly constant during inflation. If H_{inf} evolves slowly, a slight deviation of the spectral index from one is expected and indeed the observations show that that $n_s = 0.9649 \pm 0.0042$ [22].

A near scale-free $P^S(k)$ would have been generated as modes with comoving wavenumbers k successively crossed the Hubble radius and classicalized, later reentering into the Hubble horizon of the observable Universe once inflation ended. Usually no lower limit is assumed in the $P^S(k)$ spectrum so that in numerical computations of observables the integration range over Fourier modes is taken between zero and infinity.

On the other hand, a tensor power spectrum $P^T(k)$ is usually parametrized as

$$P^T(k) = A^T \left[\frac{k}{k_*} \right]^{n_T} \quad (2)$$

where the tensor spectral index n_T is expected to be small but not vanishing.

From Eqs. (1) and (2), the tensor-to-scalar ratio r is defined as

$$r = \frac{A^T}{A^S} = \frac{P^T(k_*)}{P^S(k_*)} \quad (3)$$

Current limits on r severely constrain many models of inflation and we will later check that the tensor contributions computed in this work comply with such conditions.

II. TWO-POINT ANGULAR CORRELATION FUNCTION OF THE CMB

All three COBE, WMAP and *Planck* satellite missions have observed that the temperature angular distribution of the CMB is remarkably homogeneous across the sky, with anisotropies of order 1 part in 10^5 . This observation is in fact one of the main arguments in favor of an inflationary scenario in cosmology to solve the so-called horizon problem, together with the flatness and monopole problems [23].

A powerful test of these fluctuations relies on the two-point angular correlation function $C(\theta)$ ¹, defined as the ensemble product of the temperature differences with respect to the average temperature T_0 from all pairs of directions in the sky defined by unitary vectors \vec{n}_1 and \vec{n}_2 :

$$C(\theta) = \left\langle \frac{\delta T(\vec{n}_1)}{T_0} \frac{\delta T(\vec{n}_2)}{T_0} \right\rangle, \quad (4)$$

where $\theta \in [0, \pi]$ is the angle defined by the scalar product $\vec{n}_1 \cdot \vec{n}_2$.

The information contained in the angular power spectrum of the CMB is basically the same as in the correlation function, but the latter highlights the behaviour at large angles (small ℓ) where a sizable disagreement between theoretical expectations and observations has been found. In this work we focus on the analysis of angular correlations searching specifically for imprints from the very early universe on the temperature fluctuations.

The temperature two-point correlation function is usually expanded as

$$C(\theta) = \sum_{\ell \geq 2} \frac{(2\ell + 1)}{4\pi} C_\ell P_\ell(\theta) \quad (5)$$

where $P_\ell(\theta)$ is the order- ℓ Legendre polynomial, and the sum extends from $\ell = 2$ since the monopole and dipole contributions have been removed from the analysis.

In the following, we will ignore the transfer function and consider only the SW effect as the main source of primary anisotropies, as expected on scales larger than $\simeq 1^\circ$. Hence, the multipole coefficients of Eq.(5) can be computed in the limit of a flat power spectrum $P^S(k)$, as

$$C_\ell^S = \frac{2N^S}{\pi} \int_0^\infty du \frac{j_\ell^2(u)}{u} = \frac{N^S}{\pi\ell(\ell+1)} \quad (6)$$

where j_ℓ is the spherical ℓ -Bessel function and N^S stands for a normalization factor (related to the amplitude A^S in Eq.(1)) to be determined from the fit to observational data.

An overall agreement between the behaviour of $C(\theta)$ and observational points can be achieved if the C_ℓ coefficients comply with the SW plateau condition ($C_\ell \sim 1/\ell(\ell+1)$ at small ℓ). However, the $\chi_{\text{d.o.f.}}^2$ resulting from the fit turns out to be quite unsatisfactory as, e.g., positive correlations arise at large angle, in contrast to the observed lack of large-angle correlations for $\theta \gtrsim 60^\circ - 70^\circ$ [13] among other anomalies [26].

III. SINGLE INFRARED CUTOFF IN THE SCALAR POWER SPECTRA

In order to improve the above-mentioned unsatisfactory fit, an infrared cutoff k_{\min} was introduced *ad hoc* to the CMB power scalar spectrum in Ref. [27], implying a lower limit u_{\min} in the integral of the multipole C_ℓ coefficients in Equation (6).

$$C_\ell^S = \frac{2N^S}{\pi} \int_{u_{\min}}^\infty du \frac{j_\ell^2(u)}{u}, \quad (7)$$

where $k_{\min} = u_{\min}/r_d$ and r_d denotes the co-moving distance to the last scattering surface. The authors of ref. [27] introduced the infrared cutoff essentially in a heuristic way whose purpose was removing the unseen (positive) correlations at large angle expected in standard cosmology. Later, a theoretical interpretation of k_{\min} was given as the first oscillation mode to leave the Planck domain [28] within a linearly expanding (without inflation) universe (see [29]).

In Ref. [30], this study was consistently extended focusing on the low- ℓ region of the power spectrum itself, providing an infrared cutoff value compatible with [27]. Furthermore, in Ref.[31] a suggestive connection between the lack of

¹ See also Refs. [24, 25] for a discussion on higher-order correlation functions.

correlation at large angles provided by k_{\min} and the odd-parity preference was shown. Indeed, the observed downward tail of the $C(\theta)$ function at large angles ($\theta \gtrsim 120^\circ$) was nicely reproduced, while keeping the good behaviour of $C(\theta)$ over the whole examined angular range, $4^\circ < \theta \leq 180^\circ$.

Notice, however, that a heuristic tuning of the multipole coefficients ($\ell \lesssim 10$) was required in Ref.[31] in order to reach a good agreement with data. In a following work [21], *two* lower cutoffs (instead of one) were introduced in the scalar power spectrum, providing the desired odd-parity preference of $C(\theta)$ but avoiding so many fit parameters.

Indeed, based on causality arguments two maximum correlation lengths ($\lambda_{\max}^{\text{even}}$ and $\lambda_{\max}^{\text{odd}}$ affecting even and odd parity multipoles respectively) were put forward in Ref.[21] in correspondence with two different boundary conditions. Then two comoving wavenumbers (k_{\min}^{even} and k_{\min}^{odd}) were defined accordingly for odd and even parity modes. The existence of such a doublet of (periodic and antiperiodic) boundary conditions was attributed to fundamental fermionic fields making up a composite inflaton [32].

Following essentially this idea, however no fermionic fields will be invoked in the present paper to get two different energy scales for the cutoffs. Rather, we will rely on a Kaluza-Klein model with an extra spatial dimension, so that appropriate boundary conditions of a scalar field (at the very early universe) would yield even and odd fields (regarding their Fourier expansion in k modes) in the observable four-dimensional universe. Moreover, a similar pattern will be assumed for tensor fluctuations contributing to the angular correlation function, to be incorporated to our analysis as a second step.

But first, let us examine a simple extra dimension model providing a theoretical framework and motivation for the phenomenological assumptions made so far, to be further developed in the subsequent sections.

IV. MODEL SET-UP IN EXTRA-DIMENSIONS

In this section we provide a specific scenario where those cutoffs would arise naturally. We will build a model in five-dimensions (5D) of space-time, which would lead to a 4D low energy theory when the fifth dimension is compactified. This compactification would lead to the appearance of 4D Kaluza-Klein modes whose spectrum would dictate the cutoffs we mentioned.

Let us assume that Nature at some high scale is five-dimensional (5D). For simplicity, let us also assume for the moment that there is no curvature and those 5D are flat. This situation would be described by a 5D Minkowski metric

$$ds^2 = dt^2 - dx_i dx^i - dz^2, \quad (8)$$

where $i=1, 2$ and 3 , and we denote with z the 5-th dimension.

The Universe appears to be 4D, though, and very precise tabletop experiments do confirm that the gravitational attraction between two objects of masses m_1 and m_2 is the one expected from Newton's gravity in 4D, namely $V(r) \propto m_1 m_2 / r$.

However, if gravity acted over a larger number of spacetime dimensions ($d = 4 + n$), the law would be modified to

$$V(r) \propto \frac{m_1 m_2}{r^{1+n}}.$$

which is not ruled out provided that the size of the extra-dimension is smaller than a few tenths of μm , see Ref. [33] for a recent and most precise limit.

Tiny extra-dimensions can arise through a process called compactification. There are various options to realize the compactification mechanism, including the presence of fluxes in Calabi-Yau manifolds. Depending on the configuration of the geometry and the fluxes, one can end up with different possibilities for a compact extra dimension.

For simplicity, let us assume that the extra-dimension is simply a segment of size L . Fields propagating in this geometry could be factorized in the so-called Kaluza-Klein decomposition. For any field, one can write their expression as follows

$$\Phi(x^\mu, z) = \phi(x^\mu) f(z),$$

where x^μ , with $\mu = 0 \dots 3$, are the 4D coordinates and z is the fifth dimension, $z \in [0, L]$.

For a scalar/fermion field in extra-dimensions, their 4D fields $\phi(x^\mu)$ would satisfy the Klein-Gordon/Dirac equation of motion and the fifth component, $f(z)$, would satisfy a wavefunction equation which depends on the geometry and boundary conditions at the two extremes of the interval. For example, the field Φ could have Neumann or Dirichlet boundary conditions, namely:

$$\begin{aligned} \partial_z \Phi|_{z=z_0} &= 0 \text{ (Neumann, or +)} \\ \Phi(z_0) &= 0 \text{ (Dirichlet, or -).} \end{aligned} \quad (9)$$

Those boundary conditions can be imposed in both extremes of the interval, at $z_0 = 0$ and $z_0 = L$, leading to different options for fields in the extra-dimension. From the 4D standpoint, these fields would appear as an infinite tower of 4D fields (Kaluza-Klein tower) with masses determined by the boundary conditions.

Fields with Neumann boundary conditions at both ends ($z = 0, z = L$) would be called $(+, +)$ and would exhibit a massless zero mode. Fields with other boundary conditions, (\pm, \mp) and $(-, -)$, would have a KK spectrum with a lowest KK state ($n = 0$) with a non-zero mass, providing an IR cutoff in their spectrum. Those four options for boundary conditions at $z = 0$ and L have different properties under the parity $z \rightarrow -z$. Indeed,

$$(+, +) \text{ and } (-, -) \text{ are } \textit{even}, \text{ and } (+, -) \text{ and } (-, +) \text{ are } \textit{odd}. \quad (10)$$

In flat geometries like the one described by the metric in Eq.(8), the mass spectrum of fields with boundary conditions $(+, -)$ and $(-, -)$ would be related as follows, $\frac{m_n^{(-, -)}}{m_n^{(+, -)}} = \frac{2n+2}{2n+1}$, where $n = 0, 1, \dots$. For these 5D fields, the lowest mass in their spectrum ($n = 0$) provides a natural IR cutoff for their physical behaviour. The IR cutoffs could be represented by a letter k_S and related by a simple factor 2,

$$\frac{k_S^{\text{even}}}{k_S^{\text{odd}}} = 2,$$

precisely the factor we would consider when evaluating their impact on the scalar two-point correlation in the CMB. Here we have labelled the field with $(-, -)$ as even and $(+, -)$ as odd, following the convention in the next sections. We have also added the subscript S to indicate the field we consider is scalar.

Besides scalar or fermion fields, spin-two fields are unavoidably present in any spacetime geometry. From the 4D standpoint, the Kaluza-Klein tower of the graviton spin-two field must contain a massless state, responsible for 4D gravity, and a tower of massive fields (KK-gravitons) with the same quantum numbers as the massless graviton.

The condition of a massless state implies that the tensor field satisfies $(+, +)$ boundary conditions. This choice determines the rest of the graviton spectrum. The massive spin-two fields would follow a 4D Fierz-Pauli lagrangian (describing a massive spin-two state) and their interactions with other species would be driven by the coupling to the stress tensor [34].

This construction can be generalized to metrics with curvature in the extra-dimension. Geometries with curvature in the fifth dimension have been employed in various applications, including the AdS/CFT correspondence [35], or in holographic approaches for QCD [36] and for electroweak interactions [37, 38]. In those more generic cases, analytic expressions of the KK spectrum cannot be obtained but in Ref. [39] closed expressions for the overall IR behaviour of the spectrum (sum rules) were derived. Also, let us mention that successful inflation could be achieved in these kinds of scenarios by assuming the inflaton is a pseudo-Goldstone boson and its potential is generated by the KK contributions of fields in the extra-dimension [40].

Moreover, one can relate the KK tower of spin-two fields, KK-gravitons, to other fields (fermions or scalars) propagating in the extra-dimension. In flat geometries, the first KK-graviton (coming from a $(+, +)$ field) would have its mass at the same value as the $(+, -)$ lowest mode of a scalar or fermion field, although this relation can be modified in the presence of curvature, typically leading to $k_T > k_S^{\text{odd}}$, as explained in Refs. [34, 41].

The second KK-graviton state could also contribute to the tensor correlations. The mass would be double of the first KK graviton, leading to a relation for the first two states in the KK-graviton spectrum $k_T' \simeq 2k_T$.

To summarise, fields propagating in an extra-dimension exhibit a 4D spectrum that depends on the geometry and the boundary conditions. The impact of these fields on 4D observables can be computed as a sum over contributions of 4D Kaluza-Klein fields. Below the compactification scale, those contributions would be dominated by the lowest KK modes, whose masses provide a natural IR cutoff. In the analysis of the CMB spectrum, we will consider that the cutoffs coming from the extra-dimensional scenario would be as follows

$$\begin{aligned} \text{Scalar cutoffs:} \quad & k_S^{\text{even}} = 2k_S^{\text{odd}}, \\ \text{Tensor cutoffs (from KK gravitons):} \quad & k_T \gtrsim k_S^{\text{odd}} \text{ and } k_T' = 2k_T. \end{aligned} \quad (11)$$

These (infrared) cutoffs will be taken into account in the next sections when computing correlation functions for the scalar and tensor perturbations.

V. DOUBLE INFRARED CUTOFF IN THE SCALAR POWER SPECTRUM

Once given in the past section a theoretical background to the existence of infrared cutoffs in the power spectra, let us introduce the same notation as in Ref.[21]

$$k_{\min}^{\text{odd/even}} = \frac{u_{\min}^{\text{odd/even}}}{r_d} \quad (12)$$

corresponding now to two infrared cutoffs (instead of one) in the scalar power spectrum.

Thus we rewrite the integral of Eq.(12) as

$$C_{\ell_{\text{odd/even}}}^S = \frac{2N^S}{\pi} \int_{u_{\min}^{\text{odd/even}}}^{\infty} du \frac{j_{\ell}^2(u)}{u}, \quad (13)$$

where the lower limits of the integral are now $u_{\min}^{\text{odd/even}} = k_{\min}^{\text{odd/even}}/r_d$, thereby affecting differently the numerical values of the odd and even coefficients (actually only at low ℓ), therefore altering the shape of $C(\theta)$.

From a best fit of $C(\theta)$ to the *Planck* 2018 data, the following values for the lower cutoffs were obtained in [21]: $u_{\min}^{\text{odd}} = 2.67 \pm 0.31$ and $u_{\min}^{\text{even}} = 5.34 \pm 0.62$. In this work we will recompute these lower cutoffs but incorporating tensor modes in our analysis, also imposing the relations from the compact extra-dimension in (11). The new numerical values for both u_{\min}^{even} (scalar) will not differ greatly from the previous ones, but tensor fluctuations will certainly contribute to angular correlations, as we shall see soon.

Let us remark by now that the improvement regarding the parity dominance (affecting the downward tail in $C(\theta)$ at large angle) resulting from the introduction of two infrared cutoffs with respect to a single one, is rather limited because the net effect is restricted to the first few multipoles: $\ell \lesssim u_{\min}$. Let us mention in this regard the so-called ellipsoidal universe [42], where only the quadrupole term is actually modified, however yielding a noticeable effect in large-angle correlations.

To overcome this drawback and extend further the influence of the lower cutoff(s) on the multipole expansion of $C(\theta)$, we will next include the contribution of (tensor) modes thereby modifying further the C_{ℓ} , reaching higher ℓ values.

VI. TENSOR MODES AND EXTRA INFRARED CUTOFFS

In this section we address the effect of primordial gravity waves generated during inflation on the CMB temperature anisotropies due to tensor modes, which constitutes the main goal of this paper. To this end, and taking into account that we are examining angular correlations, the following expression will be used to compute the tensor coefficient of the ℓ multipole according to Ref.[43]

$$C_{\ell}^T = \frac{N^T (\ell - 1)\ell(\ell + 1)(\ell + 2)}{2\pi} \int_0^{\infty} du \frac{j_{\ell}^2(u)}{u^5} = \frac{N^T}{15\pi} \frac{1}{(\ell + 3)(\ell - 2)}, \quad \ell > 2 \quad (14)$$

in an analogous way as C_{ℓ}^S in Eq.(6), where the normalization factor N^T is now related to the amplitude A^T in Eq.(2), similarly as N^S for the scalar modes.

Similarly to the scalar case and following the arguments given in Section IV, we will assume that two lower cutoffs equally apply to the above integral in Eq.(14) such that

$$C_{\ell_{\text{odd/even}}}^T = N^T \frac{(\ell - 1)\ell(\ell + 1)(\ell + 2)}{2\pi} \int_{u_{\min}^{\text{odd/even}}(\text{tensor})}^{\infty} du \frac{j_{\ell}^2(u)}{u^5} \quad (15)$$

again distinguishing odd and even modes by different lower cutoffs, satisfying the ratio $u_{\min}^{\text{even}}(\text{tensor}) = 2u_{\min}^{\text{odd}}(\text{tensor})$.

VII. PARITY STATISTIC ANALYSIS

As commented in the Introduction, a possible connection between an “odd universe” (i.e. parity-breaking) and the lack for large-angle correlations has been contemplated in the literature though without a clear theoretical explanation yet Ref.[44–47]. The deviation from even-odd parity balance in angular correlations can be studied by means of a parity statistic defined in Refs. [7, 8]

$$Q(\ell_{\max}^{\text{odd}}) = \frac{2}{\ell_{\max}^{\text{odd}} - 1} \sum_{\ell=3}^{\ell_{\max}^{\text{odd}}} \frac{D_{\ell-1}}{D_{\ell}} ; \ell_{\max}^{\text{odd}} \geq 3 , \quad (16)$$

where ℓ_{\max}^{odd} stands for the maximum odd multipole up to which the statistic is computed. Any deviation from unity of this statistic as a function of ℓ_{\max}^{odd} points to an even-odd parity imbalance: below unity implies odd-parity dominance and a downward tail at large-angle in the $C(\theta)$ plot, above one implies even-parity dominance and a upwards tail. As we will see soon, the parity statistics $Q(\ell_{\max}^{\text{odd}})$ play a crucial role in our work assessing the different contributions of scalar and tensor modes to angular correlations.

A. Physical scale of the infrared cutoffs

From our previous fits to *Planck* 2018 data, the resulting scalar infrared cutoffs (as comoving wavenumbers) turned out to be of order:

$$k_{\min} \simeq \frac{\text{few}}{r_d} \approx \text{few} \times 10^{-4} \text{ Mpc}^{-1} \rightarrow k_{\min} \simeq \text{few} \times 10^{-42} \text{ GeV} \quad (17)$$

where the last figure is expressed in GeV units, which amounts to a very low value indeed. However, physical cutoffs have to be obtained by dividing them by the scale factor, in particular at the time when compactification of the extra dimension took place (t_{extra}), likely at the very early universe. Therefore the corresponding physical wavenumber, basically set by the inverse radius of the extra dimension, has to be computed as $k_{\min}/a(t_{\text{extra}})$.

Now assuming that the time of compactification happened at some time between the end of the Planck epoch t_{Planck} and the beginning of inflation t_{init} , the respective scale factors $a(t_{\text{Planck}}) \simeq 10^{-61}$ and $a(t_{\text{init}}) \simeq 10^{-56}$ given in [48] lead to the following physical cutoff range:

$$\frac{k_{\min}}{a(t_{\text{extra}})} \in 10^{19} - 10^{14} \text{ GeV}, \quad t_{\text{Planck}} < t_{\text{extra}} < t_{\text{init}} \quad (18)$$

which interestingly contains the GUT scale.

Thus the existence of an infrared cutoff in the CMB temperature correlations is consistent with the assumption of an extra dimension with a high compactification scale.

VIII. FINAL ANALYSIS AND DISCUSSION

Let us first summarize the successive steps made in this work concerning the set of infrared cutoffs in the scalar and tensor power spectrum to improve the $\chi_{\text{d.o.f.}}^2$ of the fits to *Planck* 2018 data points.

- No infrared infrared cutoff is introduced to the scalar power spectrum, and the multipole coefficients satisfy the SW-plateau, i.e., $C_{\ell} \sim 1/\ell(\ell+1)$, $\ell \lesssim 30$.
- A single infrared cutoff k_{\min} is introduced to the scalar power spectrum corresponding to $u_{\min} = 4.5$ in the integral (7).
- Two infrared cutoffs $k_{\min}^{\text{odd/even}}$ are introduced to the scalar power spectrum yielding two lower cutoffs $u_{\min}^{\text{even}} = 2u_{\min}^{\text{odd}} \simeq 5.4$ in the integral (13).
- A set of infrared cutoffs $k_{\min}^{\text{odd/even}}$ (tensor) are further introduced to the tensor power spectrum, in addition to the scalar modes, according to the pattern: $u_{\min}^{\text{even}}(\text{tensor}) = 2u_{\min}^{\text{odd}}(\text{tensor})$, as theoretically motivated in section IV.

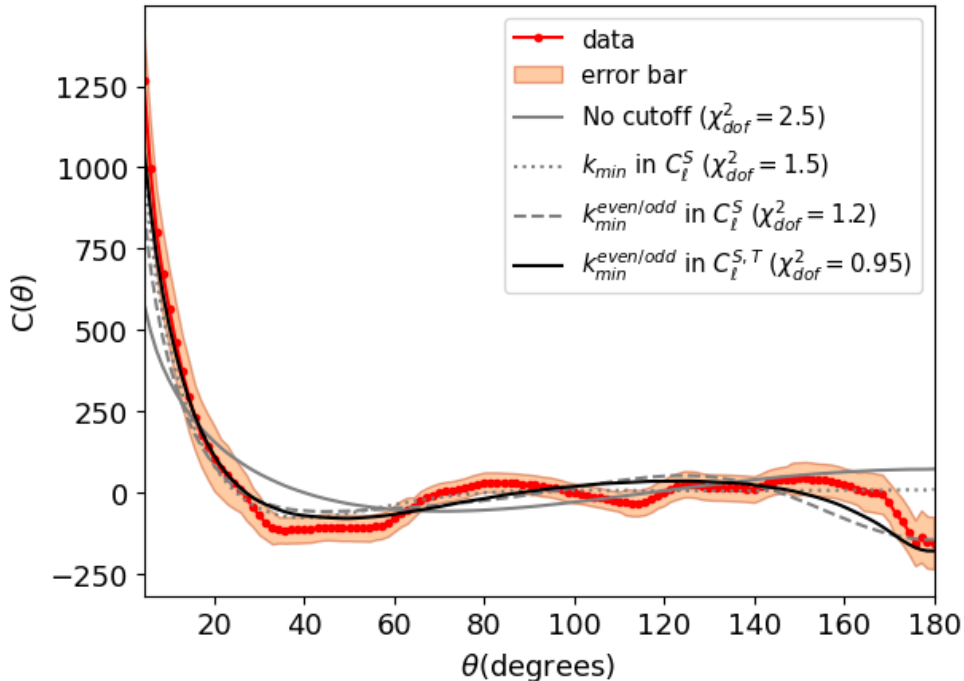


FIG. 1. Temperature 2-point angular correlation function as a function of θ from the fit to *Planck* 2018 data, for the four different assumptions discussed in the text. The shadowed area represents one σ error bar.

Figures 1 and 2 show the best $\chi^2_{\text{d.o.f.}}$ fits of $C(\theta)$ and $Q(\ell_{\text{max}})$ to *Planck* data. Let us remark that, under the conjecture that $u_{\text{min}}^{\text{odd}}(\text{tensor}) = u_{\text{min}}^{\text{even}}(\text{scalar})$, incorporating the tensor contribution in our analysis does not mean increasing the number of free fit parameters, except for the extra normalization factor N^T , in Eq.(15).

From the above fits the value of the lower cutoff $u_{\text{min}}^{\text{odd}}(\text{scalar}) = 2.5$ is extracted, while the values of all the other (both scalar and tensor) lower cutoffs become determined by the pattern associated with the compact extra dimension (i.e. multiplicative factors 2). Let us also note that this value of $u_{\text{min}}^{\text{odd}}(\text{scalar})$ is slightly smaller (but compatible within errors) than the value obtained in Ref.[21], without tensor modes.

Notice that besides the rather modest improvement of the $\chi^2_{\text{d.o.f.}}$ of the fits in Fig.q as new cutoffs are incorporated, the downward tail at large angle is only reproduced in cases (c) and (d), where the odd-parity preference can be traced back to the introduction of the set of infrared cutoffs. More clearly, figure 2 shows the increasing improvement of the fits as new cutoffs are successively incorporated to the fit. It is interesting to note that the inclusion of tensor modes especially improves the agreement in the interval $10 \lesssim \ell \lesssim 30$.

IX. SUMMARY AND DISCUSSION

We have examined angular temperature correlations of the CMB, following the trail of previous works [21, 27, 31]. We first introduced a couple of infrared cutoffs into the scalar power spectrum, thereby modifying the behaviour of the 2-point correlation function $C(\theta)$ and the parity statistic $Q(\ell_{\text{max}})$. In this way we were able to bring the model expectation closer to the *Planck* 2018 data points. However, the effect on correlations and parity balance is limited to rather low multipoles as $\ell \lesssim 6$ and the improvement finally achieved is rather modest.

Thus, in order to improve further the fits of both $C(\theta)$ and $Q(\ell_{\text{max}})$, tensor modes contributing to the CMB temperature fluctuations were included in the analysis. Let us note that the possibility of unraveling the influence of the cosmological gravitational background on the observed lack of large-angle temperature correlations in the CMB has been envisaged elsewhere, e.g., [49].

On the other hand, motivated by an extra dimension KK model, two sets of infrared cutoffs satisfying $k_{\text{min}}^{\text{even}} = 2k_{\text{min}}^{\text{odd}}$ were introduced to both the scalar and tensor power spectra. The resulting lower cutoffs $u_{\text{min}}^{\text{odd/even}}$ affect differently the $C_{\ell_{\text{odd/even}}}^{S,T}$ coefficients in the Legendre polynomial expansion of $C(\theta)$, consequently modifying the fits to angular distributions. The value of $\chi^2_{\text{d.o.f.}}$ for the $C(\theta)$ fit goes from 2.5 to 0.95, a substantial improvement with respect to

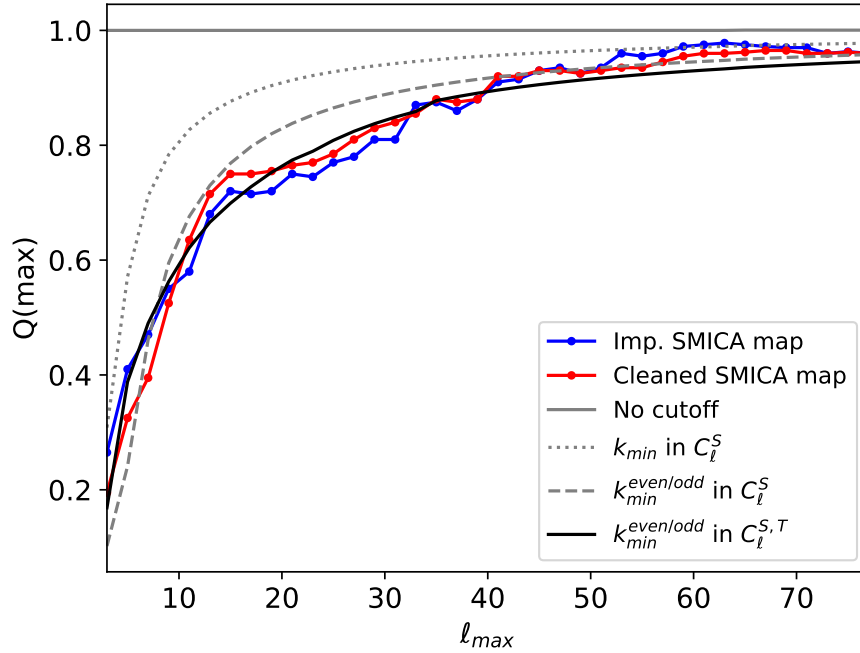


FIG. 2. Parity-statistic $Q(\ell_{max})$ versus ℓ_{max} as defined in the text under the same conditions as in caption of Fig.1, and the measured points by *Planck* (red and blue) under application of two different SMICA masks to suppress undesired foreground.

the initial assumption of no cutoff at all. Furthermore, the accordance of the parity statistic $Q(\ell_{max})$ to data largely improves, as can be seen in Fig.2.

Lastly, from our analysis we estimate the value of the tensor-to-scalar ratio r defined in Eq.(3). To do so, we employed the ratio C_ℓ^T/C_ℓ^S for different (low) ℓ 's computed from our fits of the correlation function $C(\theta)$. The following expression (from [43]) was used:

$$r \approx 0.68 \times \frac{C_\ell^T}{C_\ell^S} \quad (19)$$

Inserting now the average value $\langle C_\ell^T/C_\ell^S \rangle \simeq 0.04$ computed from our fits in the $10 \leq \ell \leq 20$ interval (where the SW-plateau is reached for both scalar and tensor modes), we get the estimate

$$r \simeq 0.027 \pm 0.003 \quad (20)$$

which lies under current limits [22]. Let us point out that the above error bar has been estimated exclusively from the dispersion of the C_ℓ^T/C_ℓ^S values obtained from our fits, while other no less important uncertainties, like the theoretical approximations and modelling dependence used throughout this paper, have not been taken into account. Therefore the above r value is mainly intended as a consistency test of our results, but not a precise determination of its value from this study. We can also cast the above result into usual slow-roll inflation parameters. For example, using $r = 16\epsilon$, we get $\epsilon \simeq 0.0017$, well within the slow-roll assumption.

As a final remark, uncertainties including the cosmic variance (not considered in this paper), a possible statistical fluke at large angles, contamination or non-cosmological effects [26, 50], or even alternative theoretical explanations [51], must certainly be kept in mind. Nevertheless, the suggestive accordance between the observed points and fits achieved when successive sets of infrared cutoffs in the power spectrum (for both scalar and tensor modes) are incorporated into the analysis, is remarkable enough to stress this way of unraveling tensor modes (from PWG produced during inflation) showing up in CMB temperature correlations, besides the usual search based on B-mode polarization.

ACKNOWLEDGMENTS

M.A.S.L. thanks interesting discussions with F. Melia and D. G. Figueroa. M.A.S.L. acknowledges support by the Spanish Agencia Estatal de Investigacion under grant PID2020-113334GB-I00 / AEI / 10.13039/501100011033, and by Generalitat Valenciana under grant CIPROM/2022/36. The research of V.S. is supported by the Generalitat Valenciana PROMETEO/2021/083 and the Ministerio de Ciencia e Innovacion PID2020-113644GB-I00.

Appendix: Even versus odd polynomials and Chebyshev polynomials

Notice the following relations between Legendre polynomials and the square of cosine functions with entire and half-entire (2π) periods playing a fundamental role in the assignments of the infrared cutoffs to even and odd multipole terms respectively:

$$\begin{aligned}
 P_1(\cos \theta) &= -1 + 2 \cos^2(\theta/2) \\
 P_2(\cos \theta) &= -0.5 + 1.5 \cos^2(\theta) \\
 P_3(\cos \theta) &= -1 + 0.75 \cos^2(\theta/2) + 1.25 \cos^2(3\theta/2) \\
 P_4(\cos \theta) &= -0.7184 + 0.6249 \cos^2(\theta) + 1.0937 \cos^2(2\theta) \\
 P_5(\cos \theta) &= -1 + 0.4687 \cos^2(\theta/2) + 0.5469 \cos^2(3\theta/2) + 0.9844 \cos^2(5\theta/2) \\
 &\dots
 \end{aligned} \tag{A.1}$$

Higher order Legendre polynomials replicate the same pattern: even and odd Legendre polynomials either contain $\cos^2[n\theta]$ or $\cos^2[(n+1/2)\theta]$ terms, to be put in correspondence with the integer and half-integer modes in the Fourier decomposition of the fluctuating field under cyclic conditions. Consequently, the infrared cutoffs $k_{\min}^{\text{odd/even}}$ apply to even and odd multipole terms respectively, in the expansion of the correlation function $C(\theta)$ in terms of Legendre polynomials. For more details see [21].

Alternatively, one can write the above relations in terms of Chebyshev polynomials $T_n(\cos(\theta)) = \cos(n\theta)$ [52]),

$$\begin{aligned}
 P_1(\cos \theta) &= T_1 \\
 P_2(\cos \theta) &= 0.25 + 0.75T_2 \\
 P_3(\cos \theta) &= 0.375T_1 + 0.625T_3 \\
 P_4(\cos \theta) &= 0.1409 + 0.3124T_2 + 0.5468T_4 \\
 &\dots
 \end{aligned} \tag{A.2}$$

Again it becomes apparent the relationship between the (even or odd) parity of the Legendre polynomials and the respective infrared cutoffs used to compute the multipole coefficients $C_{\ell \text{ even/odd}}$ through the even and odd modes of the Fourier expansion of fields.

-
- [1] C. Caprini and D. G. Figueroa, Cosmological Backgrounds of Gravitational Waves, *Class. Quant. Grav.* **35**, no.16, 163001 (2018) [arXiv:1801.04268 [astro-ph.CO]].
 - [2] C. Chiocchetta, A. Gruppiso, M. Lattanzi, P. Natoli and L. Pagano, Lack-of-correlation anomaly in CMB large scale polarisation maps, *JCAP* **08**, 015 (2021) [arXiv:2012.00024 [astro-ph.CO]].
 - [3] CORe Collaboration: Armitage-Caplan, C; Avillez, M.; Barbosa, D.; Banday, A.; Bartolo, N.; Battye, R.; Bernard, JP.; de Bernardis, P; Basak, S.; Bersanelli, M et al. CORe (Cosmic Origins Explorer) A White Paper. *arXiv* **2011**, arXiv:1102.2181.
 - [4] Young, K; Alvarez, M; Battaglia, N; Bock, J.; Borrill, J.; Chuss, D; Crill, B.; Delabrouille, J; Devlin, M; Fissel, L. et al. [NASA PICO] PICO: Probe of Inflation and Cosmic Origins. *arXiv* **2019**, arXiv:1902.10541.
 - [5] Errard, J.; Feeney, S.M.; Peiris, H.V.; Jaffe, A.H. Robust forecasts on fundamental physics from the foreground-obscured, gravitationally-lensed CMB polarization. *J. Cosmol. Astropart. Phys.* **2016**, 2016, 052.
 - [6] Copi, C.J.; Huterer, D.; Schwarz, D.J.; Starkman, G.D. Large angle anomalies in the CMB. *Adv. Astron.* **2010**, 2010, 847541.
 - [7] Aluri, P.K.; Jain, P. Parity Asymmetry in the CMBR Temperature Power Spectrum. *MNRAS* **2012**, 419, 3378.
 - [8] Panda, S.; Aluri, P.K.; Samal, P.K.; Rath, P.K. Parity in *Planck* full-mission CMB temperature maps. *Astropart. Phys.* **2021**, 125, 102493.
 - [9] Hinshaw, G.; Banday, A.J.; Bennett, C.L.; Górski, K.M.; Kogut, A.; Lineweaver, C.H.; Wright, E.L. 2-point Correlations in the COBE DMR Four-Year Anisotropy Maps. *Astrophys. J.* **1996**, 464, L25.

- [10] Bennett, C.L.; Larson, D.; Weiland, J.L.; Jarosik, N.; Hinshaw, G.; Odegard, N.; Wright, E.L. First-Year Wilkinson Microwave Anisotropy Probe (WMAP) Observations: Preliminary Maps and Basic Results. *Astrophys. J. Suppl. Ser.* **2003**, *148*, 97.
- [11] Aghanim, N.; Akrami, Y.; Ashdown, M.; Aumont, J.; Baccigalupi, C.; Ballardini, M.; Roudier, G. *Planck* 2018 results. VI. Cosmological parameters, *Astron. Astrophys.* **2018**, *641*, A86.
- [12] Akrami, Y.; Ashdown, M.; Aumont, J.; Baccigalupi, C.; Ballardini, M.; Banday, A.J.; Zonca, A. *Planck* 2018 results. VII. Isotropy and Statistics of the CMB. *Astron. Astrophys.* **2019**, *641*, A7.
- [13] Abdalla, E.; Abellan, G.F.; Aboubrahim, A.; Agnello, A.; Akarsu, O.; Akrami, Y.; Pettorino, V. Cosmology Intertwined: A Review of the Particle Physics, Astrophysics, and Cosmology Associated with the Cosmological Tensions and Anomalies. *J. High En. Astrophys.* **2022**, *34*, 49–211.
- [14] Di Valentino, E.; Mena, O.; Pan, S.; Visinelli, L.; Yang, W.; Melchiorri, A.; Mota, D.F.; Riess, A.G.; Silk, J. In the Realm of the Hubble tension: A Review of Solutions. *Class. Quantum Grav.* **2021**, *38*, 153001.
- [15] Shaikh, S.; Mukherjee, S.; Das, S.; Wandelt, B.; Souradeep, T. Joint Bayesian analysis of large angular scale CMB temperature anomalies. *JCAP08* **2019**, *2019*, 007.
- [16] Muir, J.; Adhikari, S.; Huterer, D. Covariance of CMB anomalies. *Phys. Rev. D* **2018**, *98*, 023521.
- [17] Rassat, A.; Starck, J.-L.; Paykari, P.; Sureau, F.; Bobin, J. *Planck* CMB Anomalies: Astrophysical and Cosmological Secondary Effects and the Curse of Masking. *JCAP* **2014**, *8*, 6.
- [18] Thomson, M. *Modern Particle Physics*, Cambridge University Press, 2013.
- [19] A. Lue, L. M. Wang and M. Kamionkowski, Cosmological signature of new parity violating interactions, *Phys.Rev. Lett.* **83**, 1506 (1999) [arXiv:astro-ph/9812088 [astro-ph]].
- [20] S. Alexander and N. Yunes, Chern-Simons Modified General Relativity, *Phys. Rept.* **480**, 1-55 (2009) [arXiv:0907.2562 [hep-th]].
- [21] M. A. Sanchis-Lozano, Stringy Signals from Large-Angle Correlations in the Cosmic Microwave Background?, *Universe* **8**, no.8, 396 (2022) [arXiv:2205.13257 [astro-ph.CO]].
- [22] Workman, R.L.; Burkert, V.D; Crede, V.; Klempt, E.; Thoma, U.; Tiator, L.; Agashe, K. ; Aielli, G; Allanach, B.D.; Amsler, C.D. et al. ; Particle Data Group. *Prog. Theor. Exp. Phys.* **2022**, *Prog. Theor. Exp. Phys.* 083C01.
- [23] Kolb, E.W.; Turner, M. *The Early Universe, Frontiers in Physics*; Westview Press: Boulder, CO, USA, 1994.
- [24] Gangui, A.; Lucchin, F.; Matarrese, S.; Mollerach, S. The Three-Point Correlation Function of the Cosmic Microwave Background in Inflationary Models. *Astrophys. J.* **1994**, *430*, 447.
- [25] Kamionkowski, M.; Souradeep, T. The Odd-Parity CMB Bispectrum, *Phys. Rev. D* **2011**, *83*, 027301
- [26] Zhao, W; Santos, L. Preferred axis in cosmology. *Universe* **2015**, *3*, 9.
- [27] Melia, F.; López-Corredoira, M. Evidence of a truncated spectrum in the angular correlation function of the cosmic microwave background. *Astron. Astrophys.* **2018**, *610*, A87.
- [28] Melia, F. Quantum Fluctuations at the *Planck* Scale. *EPJ-C* **2019**, *79*, 455.
- [29] Melia F. Angular Correlation of the CMB in the $R_h = ct$ Universe. *A&A* **2012**, *561*, A80.
- [30] F. Melia, Q. Ma, J. J. Wei and B. Yu, Hint of a truncated primordial spectrum from the CMB large-scale anomalies, *Astron. Astrophys.* **655**, A70 (2021) [arXiv:2109.05480 [astro-ph.CO]].
- [31] Sanchis-Lozano, M.A.; Lopez-Corredoira, M.; Sanchis-Gual, N. Missing large-angle correlations versus odd-parity dominance in the cosmic microwave background. *Astron. Astrophys.* **2022**, *10*, 142–149.
- [32] Smart, D.; Pongkitivanichkul, C.; Channuie P. Composite dynamics and cosmology: Inflation. *Eur. Phys. J. Spec. Top.* **2022**, *231*, 1325–1344.
- [33] Lee, J. G. and Adelberger, E. G. and Cook, T. S. and Fleischer, S. M. and Heckel, B. R. New Test of the Gravitational $1/r^2$ Law at Separations down to 52 μm . *Phys. Rev. Lett.* **124**, 101101 (2020).
- [34] R. Fok, C. Guimaraes, R. Lewis and V. Sanz. It is a Graviton! or maybe not. *JHEP* **12** (2012), 062
- [35] J. M. Maldacena. The Large N limit of superconformal field theories and supergravity. *Adv. Theor. Math. Phys.* **2**, 231-252 (1998)
- [36] J. Hirn and V. Sanz. Interpolating between low and high energy QCD via a 5-D Yang-Mills model. *JHEP* **12**, 030 (2005)
- [37] J. Hirn and V. Sanz. A Negative S parameter from holographic technicolor. *Phys. Rev. Lett.* **97**, 121803 (2006)
- [38] J. Hirn and V. Sanz. The Fifth dimension as an analogue computer for strong interactions at the LHC/. *JHEP* **03**, 100 (2007)
- [39] J. Hirn and V. Sanz. (Not) Summing over Kaluza-Kleins. *Phys. Rev. D* **76**, 044022 (2007)
- [40] D. Croon and V. Sanz, Saving Natural Inflation, *JCAP* **02** (2015), 008 doi:10.1088/1475-7516/2015/02/008 [arXiv:1411.7809 [hep-ph]].
- [41] B. M. Dillon and V. Sanz. Kaluza-Klein gravitons at LHC2. *Phys. Rev. D* **96** (2017) no.3, 035008
- [42] Cea, P. CMB 2-point angular correlation function in the Ellipsoidal Universe. *arXiv* **2022**, arXiv:2203.14229.
- [43] Mukhanov, V. F. *Physical Foundations of Cosmology*; Cambridge University Press: Cambridge, UK, 2005.
- [44] Land, K.; Magueijo, J. Is the Universe odd? *Phys. Rev. D* **2005**, *72*, 101302.
- [45] Kim, J.; Naselsky, P.; Hansen, M. Symmetry and Antisymmetry of the CMB Anisotropy Pattern. *Adv. Astron.* **2012**, *2012*, 960509.
- [46] Schwarz, D.J.; Copi, C.J.; Huterer, D.; Starkman, G.D. CMB anomalies after *Planck*. *Class. Quantum Gravity* **2016**, *33*, 184001.
- [47] Copi, C.J.; Gurian, J.; Kosowsky, A.; Starkman, G.D.; Zhang, H. Exploring suppressed long-distance correlations as the cause of suppressed large-angle correlations. *Mon. Not. R. Astron. Soc.* **2018**, *490*, 1–8.
- [48] J. Liu, F. Melia, Inflation with Self-consistent Initial Conditions, to be published.

- [49] G. Galloni, M. Ballardini, N. Bartolo, A. Gruppuso, L. Pagano and A. Ricciardone, Unraveling the CMB lack-of-correlation anomaly with the cosmological gravitational wave background, *JCAP* **10**, 013 (2023) [arXiv:2305.18184 [astro-ph.CO]].
- [50] Creswell, J.; Naselsky, P. Asymmetry of the CMB map: Local and global anomalies. *J. Cosmol. Astropart. Phys.* **2021**, 2021, 103.
- [51] Ashtekar, A.; Gupt, B.; Jeong ,D.; Sreenath, V. Alleviating the Tension in the Cosmic Microwave Background Using *Planck*-Scale Physics. *Phys. Rev. Let.* **2020**, 125, 051302.
- [52] Abramowitz, M.; Stegun, I.A. *Handbook of Mathematical Functions: with Formulas, Graphs and Mathematical Tables*; Dover Publications, inc., New York; 1970.
- [53] F. Melia, Tensor fluctuations in the early universe, *Astropart. Phys.* **152**, 102876 (2023).